

AD/A-001 764

THE MECHANISM OF CRAZING IN POLYSTYRENE

Stephen Wellinghoff, et al

Case Western Reserve University

Prepared for:

Office of Naval Research

25 October 1974

DISTRIBUTED BY:

**NTIS**

National Technical Information Service  
U. S. DEPARTMENT OF COMMERCE

351065

RD/A-00/764

THE MECHANISM OF CRAZING IN POLYSTYRENE

by

Stephen Wellinghoff and Eric Baer  
Department of Macromolecular Science  
Case Western University  
Cleveland, Ohio 44106

Lead instructions in  
this document may be better  
studied on microfiche.

T.R. #269

October 25, 1974

Reproduced by  
NATIONAL TECHNICAL  
INFORMATION SERVICE  
US Department of Commerce  
Springfield, VA. 22151

Approved for public release  
Distribution Unlimited

DDC  
RECEIVED  
RECEIVED

SUMMARY

The craze initiation and growth process in thin films of polystyrene has been studied via electron microscope techniques. Inhomogeneity in the surface microstructure gave rise to the formation of c.a. 300Å nuclei in which large strains were localized. These randomly distributed nuclei were even formed at the glass transition temperature in the presence of bulk shear deformation. A disk shaped microneck zone was ultimately formed by coalescence of these nuclei which was followed by cavitation and fibrillation of this zone at a critical internal hydrostatic tension. Cavity and fibril stability increased with molecular weight above the entanglement molecular weight. Although the microneck zone formed in the lowest molecular weight sample (10,000 M.W.) bifurcated by rapid crack growth, the addition of only a small weight percentage of a high molecular weight component (.2% 670,000 M.W.) induced cavitation and fibrillation.

## I. INTRODUCTION

An understanding of the macroscopic response of a polymer solid to deformation is dependent upon the elucidation of the physical and chemical structural influence on its micromechanics. The classification of such mechanical processes requires characterization of the microstructure prior to deformation. At present, unfortunately, the structure of even amorphous polymers is still rather controversial. Theories have been presented that postulate a random coil conformation in the solid state (Flory, 1953), a partially folded conformation with the same radius of gyration as the random coil (Lindenmeyer, 1972; Robertson 1965) and a completely collapsed coil (Aharoni, 1973); in sequence, intermolecular interactions range from minimum to maximum. A two phase partially ordered structure (Yeh, 1972) is conceivable with the recent highly interacting models, while a completely disordered single phase is derived from the earlier theory of Flory. Polymers with aromatic backbones such as bisphenol A polycarbonate and polyethylene terephthalate seem to fit the two phase model (Yeh and Geil, 1967; Carr et al., 1968; Klement and Geil, 1971, 1972; Neki, 1972) while unannealed atactic materials with bulky side chains are most probably disordered single phase (Wiendorf, 1974).

Amorphous polymers can plastically deform by crazing or by a bulk shearing process. Shear yielding involves a delocalized strain softening (Kramer, 1973) and subsequent localization of the

plastic deformation into shear bands that propagate at approximately a 45° angle to the maximum principal stress (Argon, 1973). This mode of deformation predominates in polymers with bulky main chains such as polycarbonate and polyethylene terephthalate. Only at temperatures slightly below the  $T_g$  or in the presence of environmental stress crazing agents is crazing profuse in these materials (Kastelic and Baer, 1973; Kambour, 1973). Strain softening is a co-operative bulk phenomenon (Andrews, 1969) that occurs either at a well defined creep delay time (Ender, 1968) or when the elastic strain energy reaches a critical value which is a function of strain rate, temperature, and the physical state of the material. Argon (1973) has generated the most successful theory of shear yield to date, based totally on elastic continuum considerations, thus avoiding many of the complicating aspects of the polymer solid state structure.

Of ultimate importance in polymer fracture, however, is the crazing process. This form of plastic deformation always initiates at a phase boundary under tensile stress states. Plastic deformation is localized into a narrow disc shaped zone which propagates in a direction perpendicular to the maximum principal strain (Bowden and Oxborough, 1973). Under a tensile stress state polymers with bulky side chains, such as polystyrene and poly-t-butyl styrene, craze over the entire temperature range encompassing  $T_g$  and liquid nitrogen temperatures, even when environmental effects are precluded by testing in a helium

atmosphere (Wellinghoff, 1974). Recently two excellent review articles have been published on this aspect of deformation morphology (Kambour, 1973; Rabinowitz and Beardmore, 1972). Theories of craze initiation have been developed by Rusch (1969, 1970), Gent (1970, 1972), and Argon (1972). All these theories, in their present stage of development, need refinement in order to account for the experimental observations presented here. Rusch has proposed that there exists a critical strain for crazing which is dependent on the level of frozen free volume which is initially homogeneously distributed in the bulk of the material. The imposed dilatant strain then adds sufficient free volume to bring the solid to a state characteristic of material at the glass transition temperature. A test of this model with PMMA seemed to give good agreement. However, this model fails in predicting the craze initiation strain of PS since it neglects stress concentrations and the fact that crazing is a surface activated process. Gent also considers that craze initiation results from the lowering of  $T_g$  to the test temperature under the applied dilatent stress. The material is softened locally to the rubbery state under the action of the stress concentration at an inhomogeneity. This theory requires that crack like stress concentration pre-exist in the solid prior to deformation and that the glass to rubber transition occurs at the crack tip. In this work, crazes were even found in solvent cast polystyrene films; and high angle platinum-carbon shadowing

of such films showed that defects greater than  $20\text{\AA}$  in size did not exist indicating that craze nucleation apparently is a result of the inherent surface microstructure of the material. Argon assumes that generation of microporosity and microvoid expansion under the imposed stress are responsible for craze initiation. However, a rather unusual reciprocal octahedral shear stress dependence of the activation energy for microporosity production is assumed which has yet to be critically tested. Clearly a better picture of the morphological sequence of events determining craze initiation and growth is required for future theoretical models.

Kambour and Russell (1971) and most recently Beaham et. al (1973,1972,1971) have investigated the morphology of crazes in polystyrene by electron microscopy. Beaham and coworkers, making use of both microtomed sections of restressed bulk crazes and thin films crazed directly in the electron microscope succeeded in relating the mature craze fibrillar structure to the fracture processes that occur in large samples. Employing thin film techniques, Brady and Yeh have (1973) also observed the mature craze microstructure and has attempted to demonstrate similarities between shear band and craze morphologies.

All the electron microscope work mentioned above has predominantly concerned itself with mature craze morphologies. In order to understand the specific influences of both physical and chemical structure on the failure mechanisms in a glassy polymeric solid, the present authors showed that a study of the

craze initiation morphology in thin films would be most useful (Wellinghoff and Baer, 1973). In this paper the entire microdeformation sequence responsible for craze initiation, growth, and fibrillation will be characterized in thin films of polystyrene as a function of molecular weight and temperature.



## 2. EXPERIMENTAL

### 2.1 Production and Characterization of Thin Films

Thin films (500-6000 Å thickness) of narrow fraction atactic polystyrene ( $M_w/M_n \sim 1.05$ ) were solution cast from dilute (0.1 - 0.3%) xylene solutions onto Mylar substrates held between the jaws of a manual uniaxial tensile stretcher. By heating the entire assembly at 5°C above the glass transition temperature under a stream of  $N_2$  for 4 hours, sufficient adhesion resulted to provide complete strain transfer. Selected samples were decorated with gold in order to define localized areas of microdeformation on the surface. After thermal equilibration at the deformation temperature (25°C,  $T_g - 25^\circ\text{C}$ ,  $T_g$ ), the sample was deformed to predetermined strains of 10%, 25%, and 30% at a strain rate of approximately  $10^{-2}$ /sec. After straining, the sample was held for 5 minutes and then backed with a carbon layer at room temperature to insure dimensional stability prior to stripping from the substrate with polyacrylic acid (PAA). Then this sandwich structure was floated on water to remove PAA and picked up on a grid for electron microscope observation.

In order to accurately measure the thickness of the films the following procedure was employed. The crazed carbon backed polystyrene film was picked up carbon face down on a carbon coated glass slide and a series of scratches were made with a razor blade through the combined thickness of the polystyrene and adhering carbon films.

After Pt-C shadowing at 45° incidence and additional carbon coating, the assembly was stripped by PAA and finally picked up on a grid for observation. As no shadow pileup was observed on the matrix side of the scratch edge, this procedure enabled the density of crazes to be determined as a function film thickness.

## 2.2 Effect of Film Thickness

The deformation morphology in thin films can be examined in detail over a wide range of strains by transmission electron microscopy provided that the film is strained on a supporting substrate. However, adequate comparison of crazing behavior in thin and thick films requires some knowledge of the state of strain in thin films during deformation.

Figure 1 shows two low magnification micrographs of the craze field produced by the equivalent straining of two P.S. films of differing thickness. The regular spacing between crazes is quite evident in both micrographs as is the higher density of crazes in the thin sample. This regular spacing of crazes has also been observed in bulk samples of PMMA (See Kambour p. 22, 1973). Evidently only a few isolated regions, separated by distances on the order of microns, are capable of nucleating crazes initially. The crazes suspected of growing first are labeled A in both Figures (1a, 1b). At first, crazes initiate at different strains, randomly throughout the sample. However, once the craze density has become sufficiently intense, further crazing is retarded since localized surface strain has been decreased in the matrix between crazes. Subsequently, an increase in substrate strain is then required before the surface strain between crazes A can again reach the critical craze initiation strain,  $\epsilon_c$ . At this point secondary crazes B start to grow (Figure 1a). Interaction with microshear bands is undoubtedly

responsible for the irregular growth pattern usually observed with type B crazes (Bucknell, 1972). This interaction precludes continuous rapid craze growth in the plane of the film. Type B crazes are found nucleated about a line midway between type A crazes where the surface strain relaxation caused by the growth of type A crazes is minimal.

Initially, when there are no crazes in the thin polystyrene film, the principal strain in the film,  $\epsilon_m$ , is the same as that applied to the Mylar substrate,  $\epsilon_s$ , (Figure 2a). As soon as the first craze, A, (Figure 2b) is introduced, the principal elastic strain in the surface of the matrix at both X and Y unloads below the craze initiation strain,  $\epsilon_c$ , due to the high localized deformation within the craze (Figure 2c).

Although the final fibril thickness within the craze is independent of film thickness, the craze width decreases as the polystyrene film becomes thinner (Figure 1). Evidently more matrix material is drawn into the craze growing in the thick film. If the film undergoes a decrease in thickness in the path of a growing craze, the craze will correspondingly decrease in width as soon as it's tip reaches this thinner region, independent of the effect of neighboring crazes. As a consequence, it appears that the shape of the plastically yielded zone at the craze tip changes significantly with film thickness, affecting the nucleation of intense localized plastic nuclei at the craze tip which are necessary for craze propagation. More detailed discussion will be presented in the section on craze initiation.

In Figure 3 the relationship between craze density and film thickness is displayed for two molecular weights at the same substrate strain (10%). The craze densities, for both molecular weights decrease with increasing film thickness,  $L$ , since the extent of the surface strain reduction in the vicinity of a craze increases with increasing  $L$ . The craze density of 10,000 molecular weight is always the lowest because in the absence of craze fibers the surface strain at the craze edge drops to zero thus increasing the extent of strain reduction in neighboring surface regions. Perhaps this mechanism would explain the observed molecular weight dependence of craze density in bulk samples (Thomas and Hagan, 1969).

### 2.3 Effect of Substrate on Deformation Mechanism

By suitably constraining the Mylar substrate at its ends apparent Poisson's ratio's ranging between 0.3 and 0.5 could be achieved. Since the Poisson's ratio of polystyrene before yield is .33, a net compressive stress as large as one tenth the applied tensile stress could be made to act perpendicular to the draw direction by mismatch of substrate and film Poisson ratio's. Employing the critical strain craze initiation criterion of Bowden et. Oxborough (1972) for polystyrene, we calculated that such a compressive stress would increase the craze initiation stress from 6400 psi (Kambour, 1973) to about 7200 psi. In turn, using the Mohr-Coulomb yield criterion and a value of 9300 psi in pure tension (Hayward et al., 1971), the yield stress is calculated to drop to about 8000 psi. Under such a stress state, it is

reasonable to expect that the onset of shear banding could significantly modify the initiation and growth of crazes. Indeed it was found that distinct microshear bands often terminated craze growth in cases where the substrate poisson ratio approached .5 (Figure 4; arrows A,B). Poisson's ratio mismatch was precisely controlled in our experiments in order to assure reproducibility of craze initiation and growth morphologies.

### 3. RESULTS AND DISCUSSION

#### 3.1 Craze Initiation - Nuclei Formation

In this particular part of the study, the micromorphology of craze initiation was characterized, eliminating to the greatest possible extent the influence of shear banding. The effect of a compressive stress acting perpendicular to the applied tensile strain was eliminated by adjusting the Poisson's ratio of the substrate to equal that of the polystyrene ( $\nu = .33$ ) for at least 10% deformation. In addition Brady and Yeh (1971) have shown that the increase in specific volume resulting from rapid quenching of the material from above  $T_g$  to room temperature will allow shear bands to form at lower stress levels. All our craze initiation experiments involved samples that had been allowed to cool in ambient air from only five degrees above the glass transition temperature,  $T_g$ , and subsequently heated to the deformation temperature. As a result shear deformation bands did not significantly interfere with craze initiation in our thin film studies.

The structures responsible for craze initiation are characterized most clearly in a polymer deformed as its  $T_g$  (Figures 5a, b, c). Crazeing is completely suppressed at this temperature and only "nuclei" which grow to approximately  $300\text{\AA}$  are seen for molecular weights 10,000-37,000. The complete absence of gold particles within these zones and the thinning due to severe Poisson contraction indicate that large localized

biaxial surface strains on the order of 250% are present. The nuclei size distribution is larger for molecular weights 97,000-2,000,000. Generally within these zones micronecking appears to be more diffuse than in the molecular weights 10,000-37,000. Region A in Figure 7c1 shows that in some zones there seems to be only a light, diffuse thinning within regions completely devoid of gold particles while a zone exhibiting thinning and little gold particle separation can be found at arrow B. At 20% strain (Figure 5c1) the shear deformation occurring in the surrounding matrix forces the nuclei to extend in the principal stress direction and undergo thinning due to poisson contraction.

For the larger molecular weights it seems unlikely that the movement of gold particles on the surface accurately defines the strain inherent to a nuclei region. For instance strains on the order of thousands of percent would have to be postulated for region A in Figure 5c1. The only viable explanation for these observations that we are able to offer at present is similar to the microstructural model that Klement and Geil (1971) have used to explain the large gold voided areas with little or no associated thinning that they observed in their highly deformed PET samples. They postulated that molecular segments tended to aggregate and move co-operatively under the applied stress. The gold voided areas were assumed to be partially the result of large molecular aggregates that had emerged from the interior of the film under the applied strain.



This aggregate movement might be expected as the temperature of deformation approaches the  $T_g$  where long range "entanglement" effects can be found at large strains (Onogi et al., 1972). Conceivably these "entanglements" could permit co-operative movement of a large molecular aggregate.

Although Wiendorf (1974) has conclusive evidence from small angle neutron and X-ray scattering and depolarized light scattering that polystyrene molecules exist in the solid state with a  $R_G$  characteristic of a random coil and no nodular microstructure (Yeh, 1972), the inhomogeneous aggregate movement at  $T_g$  must be explained. If a totally random homogeneous polymer solid existed, one would expect the entire structure to be cooperatively linked and to deform homogeneously. Since this is not the case, either we must postulate that some short range intersegment elastic interactions disturb the long range correlation or that the microstructure is not truly random and homogeneous (Yeh, 1972, 1973; Robertson, 1965; Lyndenmeyer, 1972; Pechhold, 1971).

Some evidence for void inhomogeneities in the solid state of amorphous polymers exists. According to Haward (1970), nucleation of regions of high free volume (voids  $\sim 10\text{\AA}$ ) are possible even in a polymer at its  $T_g$  at stresses one tenth that of the yield stress. Gas sorbtion measurements (Vieth, 1966) provide evidence for c.a.  $10\text{\AA}$  holes throughout the bulk of polystyrene samples even prior to deformation.

The activation energy for segmental motion near a void would be minimized; thus such a region would be a likely place for a nucleus to form. An especially interesting point is that we are able to observe localized inhomogeneous deformation at the  $T_g$  in the first place. Clearly, the surface of the polymeric solid is not in an equilibrium state at these temperatures under the imposed strain rates. Otherwise, microvoids that would be stable enough to nucleate a local strain inhomogeneity would not exist. Metastable surface density fluctuations induced by the imposed strain rate could be postulated. However, it is not clear whether the 5 min predeformation equilibration time at the  $T_g$  was sufficient to relax microdensity fluctuations induced by the previous cooling down from  $T_g + 5^\circ\text{C}$ . Experiments are presently underway to clarify this point.

Bowden (1970) has shown that if the strain rate increases with increasing strain at constant stress (strain softening) the material is mechanically unstable and the strain within pre-existing inhomogenities will continue to diverge from the surrounding matrix with increasing strain. This plastic instability is greatest near the yield point for a constant strain rate experiment. Indeed Kramer (1973) has shown experimentally that an overall strain softening precedes the severe strain localization characteristic of microshear bands.

If strain softening is necessary for the production of a nucleus from an inhomogeneity, it must be highly localized since at low temperatures crazing occurs in the elastic region well below the yield point in the stress strain curve. Surface strain softening could occur at lower stress levels than those required for bulk strain softening simply because of the looser segmental packing arrangement in the surface Lipatov and Fabulyag (1972). In addition any developing inhomogeneity would be free to poisson contract in plane stress in the surface region, minimizing the energy of plastic deformation.

It is illustrative to note that it is not necessary for the dilatent stress to induce a free volume state characteristic of  $T_g$  in order for crazing to occur, as supposed by Rusch and Beck (1969,1970). Assuming that craze initiation must occur at or above a free volume characteristic of  $T_g$ , we find that the tensile strain required to uniformly generate such a free volume is 3.8% for  $M_w > 50,000$  deformed at  $30^\circ\text{C}$  where the physical data from a polystyrene well characterized with respect to thermal treatment is used (Rusch, 1968). This value is about an order of magnitude higher than the observed critical strain of .33% (Ziegler and Brown, 1955).

These results are all consistent with the idea that the nuclei observed in the electron microscope are the result of strain localization at microvoid inhomogeneities in the vicinity of the surface. Indeed crazes are always observed at a phase boundary.

Reference to arrows B in Figures 6a, b shows that isolated nuclei still exist at a deformation temperature of  $T_g - 25^\circ\text{C}$ . The principle difference at this temperature is the presence of crazes. Especially interesting is the existence of sub-surface ca.  $400\text{\AA}$  nuclei which have extensively cavitated in the region of equatorial stress concentration; these structures are boxed in Figure 6c. In some subsurface nuclei, the triaxial stress was so large as to induce a single large void directly in the center of the structure.

Although craze nucleation at subsurface microscopic dirt particles is known, sub-surface c.a.  $100\text{\AA}$  voids are not sufficiently large to activate crazing. This is amply shown in the box at Figure 6c where the plastic zone initiated at the equator of the nucleus penetrates only about  $50\text{\AA}$  into the matrix. Plastic strain softening is necessary for strain rate localization and subsequent nucleus generation. The plastic zone about a discontinuity is known to be quite small in plane strain (J. G. Williams, 1973) relative to plane stress. As a consequence, craze growth beneath a surface requires a large stress concentration and continuing cavitation immediately behind the advancing plastic front; both make craze nucleation from a submicroscopic discontinuity beneath the surface improbable. Thus, again, the importance of surface region microvoids is emphasized.

Zhurkov et al. (1966, 1969) have investigated the so-called "microcavitation" phenomenon in many amorphous and crystalline

polymers under creep by small angle X-ray and light scattering techniques. Working under the assumption that these structures were voids, they calculated that their diameter was on the order of  $100\text{\AA}$  in the tensile direction and about three times this size in the perpendicular direction. These structures were continuously generated under the applied stress; no unusually large spread in the distribution of sizes was reported, making it unlikely that crazing was occurring. Formation of such structures without significant crazing is characteristic of the "blushing process" that sometimes appears in the tensile deformation of polymers close to their  $T_g$  (Rosen 1964).

Interestingly enough, the concentration of zones found from Zhurkov's work was on the order of  $10^{14} - 10^{15}/\text{cm}^3$  with a slightly higher concentration near the surface. Our surface concentration of nuclei was in the same range ( $\sim 10^{15}/\text{cm}^3$  for  $M_w = 37,500$ ;  $70^\circ\text{C}$ ;  $\epsilon = 10\%$ ). However under the surface, where significant poisson contraction is precluded, only small plastic strains ( $\sim 3\%$ ) would be allowed before the large hydrostatic tension induced by the plane strain state would induce massive cavitation. These subsurface structures that we observe in the electron microscope could give rise to the scattering behavior of the c.a.  $100\text{\AA}$  voids observed in the small angle X-ray by Zhurkov.

At room temperature, the population of nuclei is greatly reduced (Figures 7) and only structures which have

apparently formed by the coalescence of many nuclei along the direction perpendicular to the applied strain are exhibited. Regions B and A in Figure 7a and the box in Figure 7b show this behavior. These structures are observed exclusively in the vicinity of the craze tip, exemplified by regions D and C in Figure 7a. Detailed discussion of this coalescence process will be deferred to section 3.2.

No molecular weight effects, either in nuclei morphology or craze initiation kinetics (Rudd, 1963; Gruner et al., 1973) were found at room temperature simply because the large interchain elastic energy stored around any moving molecular segment makes intersegmental interactions rate controlling relative to any intramolecular contribution (Argon, 1973).

Provided poisson contractions are permitted, these intersegmental elastic interactions are continually regenerated during the entire deformation. As the orientation increases both the interchain packing and the elastic energy stored around a moving segment become larger, leading to strain hardening. This explains why a stable plastic zone of 200-300% surface strain can form in a 10,000 molecular weight polymer which theoretically has no long range entanglement network. Further Argon (1973) calculates that on the order of 10 P.S. monomer units participate in the activation free volume in shear. This value is considerably smaller than the 100 units that make up the 10,000 M.W. chain and indicates that this chain is still long enough to be controlled by intersegment interactions.

### 3.2 The Coalescence Process

So far we have been concerned only with the formation of nuclei. Formation of planar anisotropic plastic zones oriented perpendicular to the major principal strain (the precavitated craze) requires that a collection of these nuclei undergo a coalescence process.

Figure 7a shows the coalescence process occurring at the tips of two 10,000 molecular weight crazes while Figure 7b shows the same process in a 97,000 M.W. polymer. It should be noticed that the formation of the nuclei does not necessarily occur at the region of highest dilatent stress concentration immediately adjacent to the nascent plastic zone, coincident with its direction of propagation. Rather this zone seems to propagate discontinuously by distinct jumps. It follows that the coalescence process of discrete nuclei must be a consequence of a mechanically inhomogeneous polymer solid state structure. One would expect a homogeneous structure to craze by an uninterrupted propagation of the plastic zone; thus the observed behavior is consistent with the expectation that there are significant density fluctuations.

In regions further removed from the zone tip (Figure 7c) the plastic zone has organized itself into a planar zone oriented perpendicular to the tensile axis. Unlike the nearly spherical nuclei which show a virtual lack of gold particles, these more well developed zones show some random dispersal of particles

within. The presence of such particles in the central regions of these zones is a further indication of the coalescence mechanism.

In order to more completely understand this process, we will attempt to draw an analogy between our case and the mechanical model of Eubanks (1954) who has calculated the elastic stress concentration to be expected for a hemispherical void inclusion on the free surface of a semi-infinite body under a tensile stress state and has shown that there is virtually no perturbation of the uniform tensile field beyond about twice the radius of the hemisphere along the axis of symmetry of the hemisphere perpendicular to the sheet plane. It is likely that the stress intensification would be localized to a similar extent on the surface in the plane of the sheet (Figure 8; arrow A). The region of yield about such a discontinuity would be even more restricted. Except for the existence of a plastic material within the surface nucleus which exerts a traction on the interior contour of the nucleus, we might draw an analogy between Eubanks' case and the nucleus.

In order for this nucleus to ultimately grow into a craze at the same stress level, it must change its shape so as to increase the extent of its stress concentration. For example an elliptical hole having the same minor axis radius as a circle but twice the major axis radius will have a yield zone that extends three times farther in the equatorial direction (See Figure 8, arrow B). Examples of this elliptical plastic



zone shape can be found in Figures (7a, regions A and B; 7b; 9)

At this point it is likely that the equitorial stress concentration would encompass a surface region capable of initiating a nucleus. The stress concentrations of these two zones would then overlapp and plastic coalescence would occur between them (Figure 8, arrow C). As the extent of stress concentration and plastic yield increases in both the x and y directions about the initial discontinuity by a continuation of this process, the extent of stress concentration will increase in the z direction also. Eventually the area of perturbation extend to the Mylar-polystyrene boundary. If the Poisson component of the stress in the z direction is large enough, debonding will occur (Figure 8). Plastic yield throughout the film thickness would be facilitated by the plane stress state thus generated (Williams, 1973). Drawing an analogy with Bowden's strain softening - shear strain localization phenomenology, we might expect localization of further tensile strain to occur within the limits of the coalesced zone already present on the free surface once strain softening throughout the entire thickness had occurred. The width of the nascent craze would now be defined and further propagation would occur in the x direction. The thicker the polystyrene film the greater the extent of coalescence in the x - y plane that would be required before the region of stress perturbation would reach the interface and, subsequently, the wider the nascent craze at the free surface. Referring to

Figure 3, we see that the craze width is always less than the film thickness. This is further proof that the extent of the outlying elastic stress perturbation (which is larger than the coalesced zone) and its intersection with the interface controls craze width in thin films. It is unclear what causes the limiting craze width that ultimately must occur as the film thickness becomes macroscopic.

As the temperature of deformation is increased toward the  $T_g$ , the percentage of nuclei coalescing to form anisotropic plastic zones is quite small. At  $T_g - 25^\circ\text{C}$  (Figure 6) crazes are still formed; but, at  $T_g$  (Figure 5), coalescence and subsequent craze formation is absent. Undoubtedly this is a result of the bulk matrix shear deformation that occurs readily at these temperatures (Haward, 1971). The bulk yield process evidently relaxes any stress concentration induced by the nuclei thus precluding the possibility of strain localization and divergence occurring in the matrix between them.

The shear yield occurring at  $T_g$  is clearly evidenced by the organization of gold particles into irregular rows (Figure 5 b;A) isotropically oriented and separated by  $200 \text{ \AA}$  or so.

The shear deformation is still heterogeneous though since any given row structure can be traced for  $300\text{-}800 \text{ \AA}$  through the surface before it disappears into another structure.

The elongation of the 2,000,000 M.W. aggregate (Figure 9c arrow A) is further evidence for this matrix shear yield.

### 3.4. Cavitation and Fibrillation

The anisotropic microneck zones we observe in the electron microscope are the precursors to the fibrillated craze structure that ultimately leads to failure. Although these micronecks are thinner and contain less coalesced material in comparison with their thick film (bulk sample) counterparts, study of void formation in these thin film structures can provide useful insight into the behavior of crazes in thick samples.

As alluded to before, both the nuclei and the anisotropic neck zone appear to have undergone significant Poisson contraction. In Figure 9, a 97,000 M.W. sample deformed 10% is shown shadowed at high angle with Pt-C. In this rather thin film (probably  $\sim 1500\text{\AA}$ ) the microyield zone density is rather high while the mature plastic zone thickness is small. Zones even on the order of  $200\text{\AA}$  in length are found to be somewhat micronecked with the step height at the zone-matrix boundary on the order of  $30\text{\AA}$ . (Figure 9, arrow A). The shadow pileup on the opposite step makes it difficult to determine the step height of the more mature zone; but it is considerably larger, at least  $100\text{-}150\text{\AA}$ . From examination of slightly thicker films (Figure 10), the cavitation process is often found to ensue shortly after the step height has reached its maximum value. At this strain the constraints imposed by the craze edges retard normal Poisson contraction. The hydrostatic tension levels within the microneck induced by this constraint are evidently sufficient for void expansion.

Thin films of styrene-butadiene block co-polymers (courtesy Dow Chemical) were solvent cast and  $\text{OsO}_4$  stained (Bucknell, 1967)

subsequent to deformation to determine if the craze-plastic zone was in a dilated state. Figures (11a, arrow A; 11b, arrow A) show that  $\text{OsO}_4$  preferentially stains both the rubber particles and the butadiene that seems to remain in the plastic zones that nucleate at these particles. The finite butadiene concentration in the matrix between rubber particles could be a result of incomplete phase separation.

Figure 11c, shows a thin film of the same material that has deformed in shear. Although the strain in these micronecked bands is probably rather high (Argon et al, 1968),  $\text{OsO}_4$  does not preferentially stain them. Although they are not conclusive these results seem to indicate that a dilated state exists within plastic zones in Figures 11a, 11b. This appears to be reasonable since the craze plastic zone can stress relax significantly only by void formation except in the vicinity of the microneck surface (see Gent and Lindly, 1958). These voids appear to be smaller than the resolution limit of the microscope ( $<20\text{\AA}$ ).

Figure 12b shows a well developed microneck that has developed in a 2,000,000 M.W. polymer. As we proceed from the bottom to the top of the micrograph, the hydrostatic tension within the microneck reaches a critical value where rapid microvoid expansion is possible and a spherical void of about  $200\text{\AA}$  diameter forms directly in the center of the microneck zone; this is also the location of initial cavitation in 670,000 M.W. polymer. The largest triaxiality occurs about the plane farthest removed from

both free surfaces (Gent, 1958). Thus cavitation would be expected to ensue deep within the interior of the microneck. Figure 7c shows this clearly for a 97,000 M.W. polymer; cavitation first occurs near the edge of the craze under a large group of surface Au particles. The 97,000 M.W. plastic neck zone shows a facilitated propensity for cavitation with respect to 650,000 and 2,000,000 M.W.; cavitation often can occur in this polymer even before the coalescence process is complete (Figure 7b). Stable spherical microcavities did not form in the 37,000 M.W. polymer; any void that nucleated apparently grew rapidly between both craze faces parallel to the major principal stress (Figure 13a).

Spherical microcavities were not formed in the plastic zone of the 10,000 M.W. sample. Rather a region more transparent to the electron beam first initiated in the middle of the plastic zone between craze faces at a critical strain. This zone then subsequently fractured forming a crack that bisected the plastic zone (Figure 7a). The only instances of fiber formation were seen in the vicinity of a coalescence boundary where cracks from both adjacent plastic zones stopped growing (Figure 7a; region E). In some cases a microneck would form across the middle of this bridge of material leading ultimately to fracture or the formation of a fibril. This fibril would elongate only if it had been under a rather low plastic strain initially.

At the large strains and dilated state within the craze plastic zone, long range effects evidently become important.

According to Argon (1972), in order for a localized assembly of microvoids to grow by plastic deformation the rate of decrease of the hydrostatic boundary stress with expansion of the region (largest decrease for initially high porosities) must not exceed the decrease in the tension required to expand the region as it becomes larger. Although the resistance to deformation might be lower for 10,000 M.W. due to the relative lack of long relaxation times, the molecular mobility within the neck is higher and the hydrostatic tension applied to any porous region lower at the local strain rates. The critical hydrostatic tension necessary for void expansion is not obtained in this molecular weight and auto catalytic fracture occurs about a plane midway between the craze faces where the maximum principal stress (and the stress on each bond) is the largest.

At some molecular weight between 10,000 - 37,500, the molecular mobility becomes small enough so that the critical hydrostatic tension is attained and unstable growth of individual voids across the entire microneck occurs. As the mobility further decreases upon increase in molecular weight, small voids seem to be stabilized by strain hardening at their boundaries with the surrounding material.

As can be seen from comparison of Figures (12 b,c) and Figures (13a,b), increasing the temperature from room temperature to  $T_g - 25^\circ\text{C}$  has quite a drastic effect upon both the cavitation properties of the plastic zone and the ultimate stability of the fibrils. In the case of 37,000 M.W. both the density of

fibrils and the distribution of fibril diameters is larger at 25°C (30-150Å) than it is at 70°C (120-150Å). Only a few interfibrillar 30Å crosslinks are present at room temperature while they are completely absent at 70°C.

A particularly interesting feature is the process by which c.a. 150Å fibrils are formed from 400-1000Å wide precursor micronecks. Due to the relaxation and subsequent material densification that undoubtedly occurs at the free surfaces of the neck edges after their formation, yield zones nucleate about 150Å in from both of these edges in the zone of maximum constraint adjacent to the craze-bulk interface (Figure 13b; arrow A). In zones less than 500Å in width the yield generally coalesces in the center and grows through the entire length of the neck parallel to the maximum principal stress since the yield stress is undoubtedly lowest perpendicular to this direction. The lateral strain relaxation incurred by the formation of yield zones in a neck greater than 600Å diameter evidently allows material within the center of the neck to harden and densify, whereupon, three nascent fibrils are formed (13b; arrow B) instead of the usual two. The yield zone eventually cavitates and isolates the fibrils from one another (Figure 13b; arrow C).

At this temperature ( $T_g$  - 25°C) and molecular weight, fibers less than 150Å diameter are not stable and break without splitting further. Both high molecular weight and lower temperatures promulgate a continuation of this process down to the 50Å fibril diameter level, no doubt assisted in part by the lateral restraint



maintained by the crosstie fibers. It is likely that the fibrillation process described above has generality irregardless of molecular weight or temperature. One of the factors determining the final fibril diameter is undoubtedly the rate at which the material densifies and hardens in the vicinity of the free surface formed next to a cavity.

Beahan et al (1972) have observed that an increase in both the strain rate and strain induces thick  $500\text{\AA}$  fibrils to split into c.a.  $100\text{\AA}$  fibrils more readily in deference to homogeneous extension of the larger structures. These observations are consistent with our fibrillation mechanism discussed above. In order for a yield zone to form in a c.a.  $500\text{\AA}$  wide neck, the overall strain rate must be large enough to promote inhomogeneity in the local strain rate (see Bowden and Raha, 1970; Kramer, 1970, 1972). At high strain rate and low temperature the neck structure is effectively less mobile and would be expected to form a high density of localities with high strain rate (yield zones), isolating many areas of low mobility between (nascent fibers). Increasing the uniaxial orientation within the neck would assure that the yield zones would propagate quickly parallel to the principal stress with the subsequent formation of long thin fibers with few crosslinks.

To explore further the effect of molecular weight on the cavitation and fibrillation processes, binary mixtures of 670,000/10,000 M.W. were made in 1% to 0.05% weight percent of the high molecular weight component. In most cases the two fractions

were mixed in xylene and evaporated in the normal fashion. Another polymer blend from tetrahydrofuran solution was shock precipitated into water, the precipitate melted onto mylar, and the resultant samples compared in order to determine the homogeneity of the mixture. No difference in craze morphology was found between the two methods.

The 1% material cavitated in a fashion similar to that observed in a 37,000 M.W. with void nucleation usually initiating at the craze matrix boundary, subsequently giving rise to the fiber morphology shown in Figure 14a. Even at this low percentage of high molecular weight component some cross-links are visible.

Decreasing the high molecular weight component to the 0.5% to 0.1% range induces the plastic zone to initially form a neck down the center of the plastic zone (Figure 14D); however, cracks do not nucleate in this neck and completely split the plastic zone as in monodisperse 10,000 M.W. Rather secondary yield zones are found to branch from this central region and grow toward the craze-matrix boundary (14D; arrow A). Any cracks that do form grow only short distances laterally, often not completely through the thickness of the neck. As a result, because some strain hardening capacity exists in the principal stress direction, a fiber type morphology forms even at 0.2% (Figure 14B). Between weight percentages of 0.1-0.05% the entire cavitation and fibrillation process is indistinguishable from that of the 10,000 M.W. and few or no fibers form (Figure 14c).

Murakami et al. (1971) have observed from stress relaxation experiments carried out above  $T_g$  that mixing 50% 10,000 M.W. into a binary mixture with 500,000 M.W. eliminates about 40% of the rubbery relaxations of the high molecular weight component, and shifts the maximum relaxation time by three orders of time. Onogi et al (1972) show that a 60% mixture of 600,000 M.W. with a 25,000 M.W. component reduces the fracture strain by some 50% and the fracture stress by an order of magnitude for low strain rates above  $T_g$ . From these experiments it was concluded that low molecular weight components have a very strong effect on the long relaxation times and act simply as a plasticizer for the HMW component. Based on these results we should expect that 99%-99.9% low molecular weight material (10,000) should all but eliminate the rubbery region of the HMW component.

If we assume for the moment that each molecule has the random coil dimensions in the solid state, each 670,000 M.W. molecule would overlap at its  $R_g$  at about .15 wt.% (random coil dimensions assumed same as in butanone 22°C, Ferry, 1961). Using the gaussian coil segment distribution, we calculate that each 100Å cube in the vicinity of  $R_g$  to contains between 60 HMW monomer units. Further, if each of these units belongs to the same chain and this chain is fully extended, just about one chain joining HMW molecules could bridge the cube from fact to face. This certainly is much less than the density of interpenetrations usually required for entanglement. The uniform density models of Aharoni and Lindenmeyer would predict even fewer interactions between HMW molecules.

Evidently "entanglement" type interactions are not completely necessary for fiber formation. However, very small percentages of high molecular weight apparently modify the ultimate plastic flow properties of the 10,000 M.W. material so that some orientation hardening is possible, precluding the formation of a crack in the middle of the plastic zone.

#### 4. CONCLUSIONS

The surface microstructure of thin films of polystyrene was found to be sufficiently heterogeneous to initiate localized strain inhomogeneities of c.a.  $300\text{\AA}$  diameter. These nuclei were found even at the glass transition temperature where the predominant mode of deformation was a bulk shear process that was heterogeneous on the  $500\text{\AA}$  level. The correspondingly larger sizes and more delocalized deformation found for nuclei formed in the 2,000,000 M.W. polymer at  $T_g$  provided evidence for molecular aggregate movement at this temperature.

At temperatures below the glass transition these nuclei grew into a more elliptical shape which induced a stress concentration in the surrounding matrix that was sufficient to initiate additional nuclei nearby. The subsequent overlap of stress concentrations promoted a coalescence of the two zones along the minor principal stress direction in the surface. A repetition of this heterogeneous nucleation and coalescence process ultimately led to the formation of narrow disk shaped microneck zones propagating perpendicular to the applied strain.

Although no voids greater than  $15\text{\AA}$  were found in the microneck zone,  $\text{OsO}_4$  staining experiments showed that the microneck was likely to be in a dilated state. When sufficient hydrostatic tension was generated within the neck by the constraints of the craze edges, c.a.  $100\text{\AA}$  cavitation ensued. Although polymers of differing molecular weight exhibited no qualitative morphological differences in their nucleation and coalescence processes, the molecular weight was found to exert a large effect upon the cavitation process that immediately proceeded fibrillation. When the molecular weight was significantly below the entanglement molecular weight (e.g. 10,000 M.W.), void expansion and fiber formation did not take place. Instead rapid crack growth bifurcated the plastic zone. Significant void growth and fiber formation was first observed with molecular weight above the critical entanglement molecular weight. Very small amounts of high molecular weight polymer were required to induce void expansion and fibril formation in the 10,000 M.W. polymer demonstrating that entanglements in the usual sense were not responsible for the reinforcement of the microneck.

ACKNOWLEDGEMENTS

We wish to thank the Goodyear Tire and Rubber Company for its fellowship support of S. Wellinghoff and the Office of Naval Research for its generous financial support of this work.

REFERENCES

- S. M. Aharoni, J. Macromol. Sci. -Phys., B7(1), 73 (1973).
- R. D. Andrews, ACS Polymer Preprints, 10(2), 1110 (1969).
- A. S. Argon, paper presented at U.S. - Japan Joint Seminar on the Polymer Solid State in Cleveland, Ohio, October 9-13 (1972); to be published in J. Macromol. Sci. (1974); Phil. Mag., 28, 839 (1973).
- A. S. Argon, R. D. Andrews, J. A. Godrick, and W. Whitney, J. Appl. Phys., 39(3), 1899 (1968).
- P. Beahan, M. Bevis, D. Hull, J. of Materials Sci. 8, 162 (1972); Polymer 14, 96 (1973); Phil. Mag. 24, 1268 (1971).
- P. B. Bowden and R. J. Oxborough, Phil. Mag. 28, 547 (1973).
- P. B. Bowden and S. Raha, Phil. Mag. 22, (177), 455, 463 (1970).
- T. E. Brady, G.S.Y. Yeh; Journal of Materials Sci. 8, 1083 (1973); J. Macromolecular Sci. -Phys., B7(2), 243 (1973); Journal of Appl. Phys., 42(12), 4622 (1971).
- C. B. Bucknall, D. Clayton, and W. E. Keast, Journal of Materials Sci. 7, in press (1972).
- C. B. Bucknall, British Plastics, 40, 84 (1967).
- S. H. Carr, P. H. Geil, and Eric Baer, J. Macromol. Sci.-Phys. B 2(1), 13 (1968).
- D. Ender, J. Appl. Phys., 39(11), 4877 (1968).
- R. A. Eubanks, J. Appl. Mech., 21(1), 57 (1954).
- J. D. Ferry, Viscoelastic Properties of Polymers, John Wiley and Sons Inc., New York (1961).
- P. J. Flory, Principles of Polymer Chemistry, Cornell Univ. Press, Ithaca, N. Y., 402-409, 426-431 (1953).
- A. N. Gent, J. of Materials Sci. 5, 925 (1970).
- A. N. Gent and A. G. Thomas, J. Polymer Sci., Part A-2, 10, 571 (1972).
- A. N. Gent and P. B. Lindley, Proc. Royal. Soc. (London), A249, 195 (1958).
- C. L. Gruner and R. P. Kambour, unpublished work.

- R. N. Haward, B. M. Murphy, E. F. T. White, J. of Polymer Sci., A-2(9), 811 (1971).
- R. N. Haward, presented at Int. Symposium on the Phys. of Non-crystallized Solids, Sheffield, England, September 14-18 (1970).
- R. P. Kambour, Journal of Poly. Sci., Part D, to be published 1973; also G. E. Report #72CRD285, October (1972).
- R. P. Kambour and R. R. Russell, Polymer 12, 237 (1971).
- J. Kastelic and Eric Baer, J. Macromol. Sci-Phys., B7(4), 679 (1973).
- J. J. Klement and P. H. Geil, J. Macromol. Sci-Phys, B6 (1), 31 (1972); B5, 505, 535 (1971).
- E. J. Kramer, J. Appl. Physics, 41 (11), 4327 (1970); Report #2030, Materials Science Center, Cornell University (1973).
- E. J. Kramer and R. C. Richards, J. Macromol. Sci.-Phys., B6 (1), 229 (1972).
- P. H. Lindenmeyer, J. Macromol. Sci.-Phys., B8, 361 (1963).
- Yu S. Lipatov and F. B. Fabulyak, J. Appl. Poly.Sci.16(8), 2131 (1972).
- K. Murakami, K. Ono, K. Shiina, T. Ueno, M. Matsuo, Polymer Journal, 2 (6), 698 (1971).
- K. Neki, Ph.D. Thesis, CWRU (1972).
- S. Onogi, T. Matsumoto, E. Kamei, Polymer Journal, 3 (5), 531 (1972).
- W. Pechhold, Journal of Poly. Sci., Part C, Polymer Symposium, 32, 123 (1971).
- S. Rabinowitz and P. Beardmore, Critical Reviews in Macromol. Sci., CRC Press, March 1972.
- R. E. Robertson, J. Phys. Chem. 69, 1575 (1965).
- B. Rosen, Fracture Processes in Polymeric Solids, Interscience, New York (1964).
- J. F. Rudd, J. of Polymer Sci., Part B, 1, 1 (1963).
- K. C. Rusch and R. H. Beck, Jr., J. Macromol. Sci.-Phys., B3(3), 365 (1969); B4(3), 261 (1970).
- K. C. Rusch, J. Macromol. Sci.-Phys., B2(3), 431 (1968).



D. P. Thomas and R. S. Hagan, Polymer Eng. Sci., 9, 164 (1969).

W. R. Vieth, P. M. Tam, A. Michaels, J. Colloid and Interface Sci.; 22(4), 360-370 (1966).

S. Wellinghoff and Eric Baer, Handbook of the Second International Conference on Fracture and Yield, Cambridge, England (1973); to be published (1974).

Wiendorf, private communication (1974).

J. G. Williams, Stress Analysis of Polymers, Longman, London, 255-256 (1973).

G. S. Y. Yeh, J. Macromol. Sci.-Phys., B6(3), 451 (1972); B6(3), 465 (1972). Critical Reviews in Macromol. Sci. I(2), 1 (1972).

G. S. Y. Yeh and P. H. Geil, J. Macromol. Sci., Phys. B1(2), 235 (1967).

S. N. Zhurkov, Proc. First Int. Conf. on Fracture (Sendai), Y. T. Yokoboni, et al. editors, Japan Soc. Strength Fract. Mater., Sendai, Japan, p. 1167.

S. N. Zhurkov, V. S. Kuksenko, A. I. Slulsken (1969), in Fracture 1969, (P. L. Pratt, et al. editors), Chapman and Hall, Ltd. London p. 531.

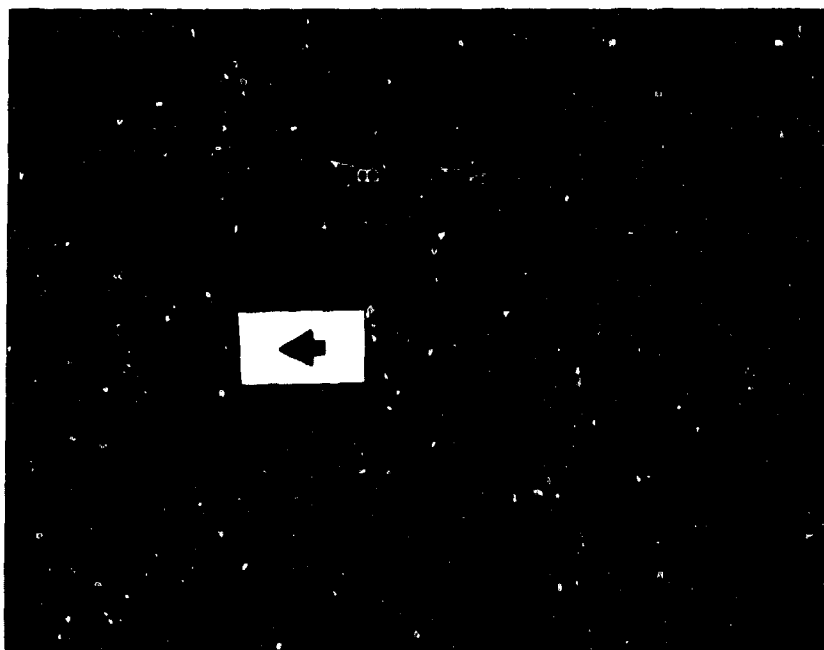
S. N. Zhurkov, V. I. Vettegren, V. E. Korsukov, and I. I. Novak, (1969), Fracture 1969, p. 545.

E. E. Ziegler and W. E. Brown, Plastics Technol., 1, 341, 409 (1955).

FIGURE CAPTIONS

- 1a. Electron micrograph of 3000Å thick film of 2.5/1 mixture of 670,000/10,000 deformed 25% showing types A and B crazing. Sample annealed 81°C 20 days. Poisson ratio substrate  $\nu$  .33 (C coat only; arrow in tension direction).
- 1b. Same as 2A, except 6000Å thick, showing decreased craze density and increased craze thickness.
2. Schematic showing the normal stress attenuation characteristics to be expected in the substrate surface parallel to the applied tensile stress in the vicinity of the craze boundary.
3. Graph of craze density vs. film thickness for two molecular weights ( $\diamond$ ) and craze width vs thickness for one molecular weight ( $\bullet$ ) (Substrate strain 10%).
4. Electron micrograph of  $\sim$ 5000Å thick film of  $M_w = 2,000,000$  deformed 25% on a Mylar substrate. Poisson ratio substrate  $\nu$  .43; sample  $\nu$  .33. Slow cooled from  $T_g$  (Carbon coat only).
5. Electron micrographs showing three molecular weights deformed at  $T_g$ . Crazing is completely suppressed at this temperature (Au decoration prior to 10% deformation, C coat).  
A- $M_w = 10,000$ ,  $T_g = 83^\circ\text{C}$ ; B- $M_w = 37,500$ ,  $T_g = 95^\circ\text{C}$ ;  
C 1  $M_w = 2,000,000$ ,  $T_g = 100^\circ\text{C}$ ; C 2 same as C 1, 20%).
6. Electron micrographs showing three molecular weights deformed at  $T_g - 25^\circ\text{C}$ . A significant decrease in the coalescence tendency of the microyield zones is found (Au decoration prior to 20% deformation, C coat)  
A- $M_w = 10,000$ ,  $T_{\text{deform}} = 58^\circ\text{C}$ ; B- $M_w = 37,500$ ,  $70^\circ\text{C}$ ;  
C- $M_w = 2,000,000$ ,  $75^\circ\text{C}$ .
7. Electron micrograph showing the microyield phenomenon and the coalescence process leading to craze nucleation.  
(Au decoration prior to 10% deformation, C coat) A- $M_w = 10,000$ ;  
B, C- $M_w = 97,200$ ; D- $M_w = 2,000,000$ ; E-Blank (no deformation).
8. Schematic showing qualitatively the stress concentrations to be expected around the surface discontinuities responsible for craze initiation.
9. Electron micrograph of  $M_w = 97,200$  film deformed 10% showing the micronecking behavior of nascent crazes and microyield zones (Pt-C shadow) =  $14^\circ$ , C coat).
10. Electron micrograph of  $M_w = 97,200$  deformed 10% showing a region where the step height has become constant in the vicinity of the ensuance of cavitation ( $14^\circ$  Pt-C shadow angle; Au decoration prior to shadow and deformation; insert at higher exposure).


- 11a. 70/30 styrene-butadiene block copolymer solvent cast from THF and annealed 4hrs at 105°C (17% deformation, Poisson ratio substrate = .33, OsO<sub>4</sub> 10% solution 1hr, C coat).
- 11b. Same as 15a except solvent cast from xylene at 110°C and annealed 10hrs at 105°C.
- 11c. Same as 15a except annealed at 110°C-2hrs and 101°C 8hr (Poisson rate substrate = .45).
- 12a. Cavitation and fibril formation in a  $M_w = 670,000$  deformed at room temperature (C coat).
- 12b. Same as a except  $M_w = 2,000,000$ .
- 12c. Same as b except  $T_{\text{deform}} = T_g - 25^\circ\text{C}$ .
- 13a. Dense fibril morphology in a  $M_w = 37,500$  deformed at room temperature (C coat).
- 13b. Same as a except at  $T_g - 25^\circ\text{C}$ .
- 14a. 1.0% binary mix of 670,000/10,000 deformed at room temperature (C coat).
- 14b. Same as A, 0.2%.
- 14c. Same as A, 0.05%
- 14d. Same as A, 0.05% (Au decoration prior to deformation).

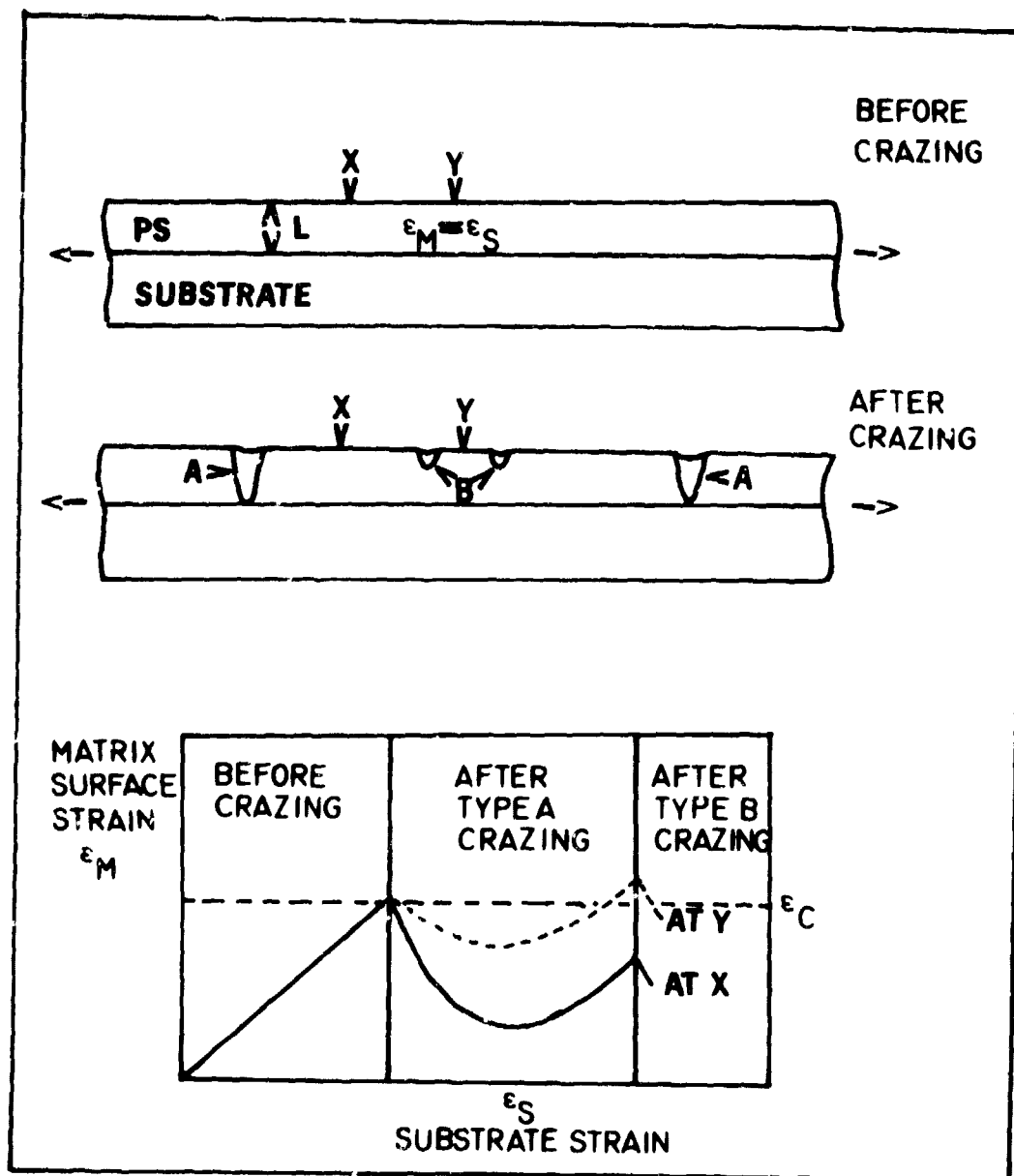


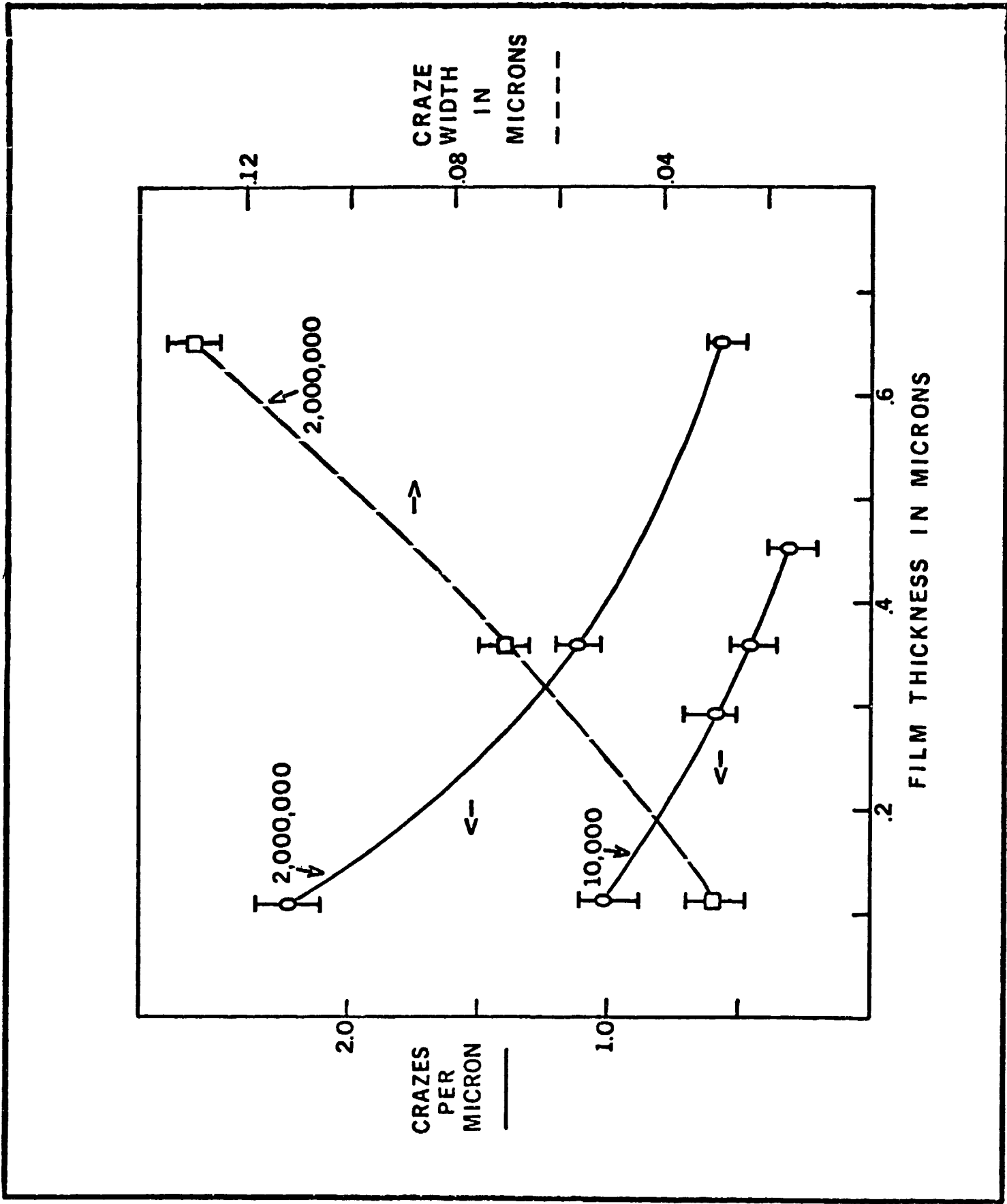
1A



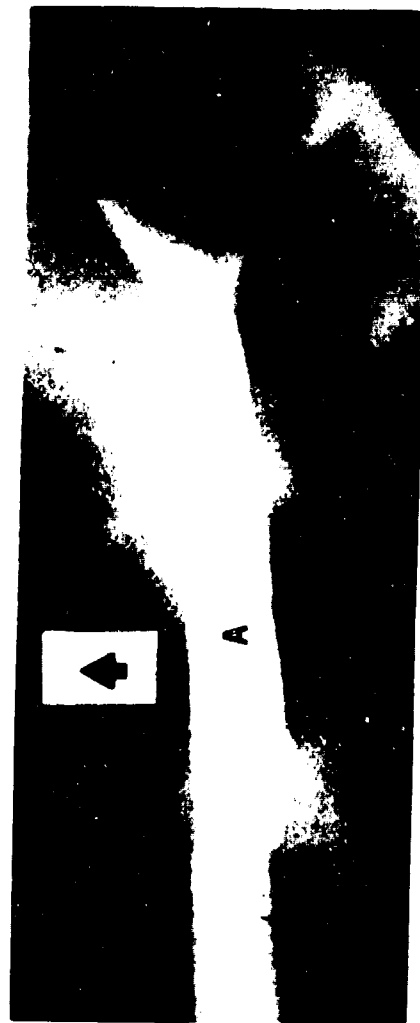
1B

 .5μ





4



.3μ





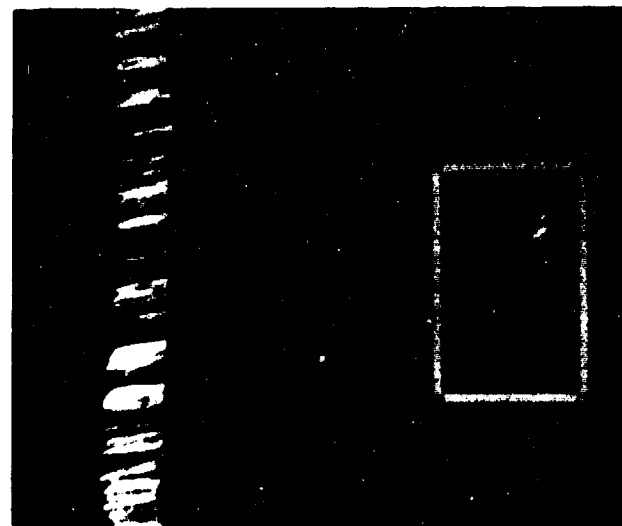
6A



6B



6C

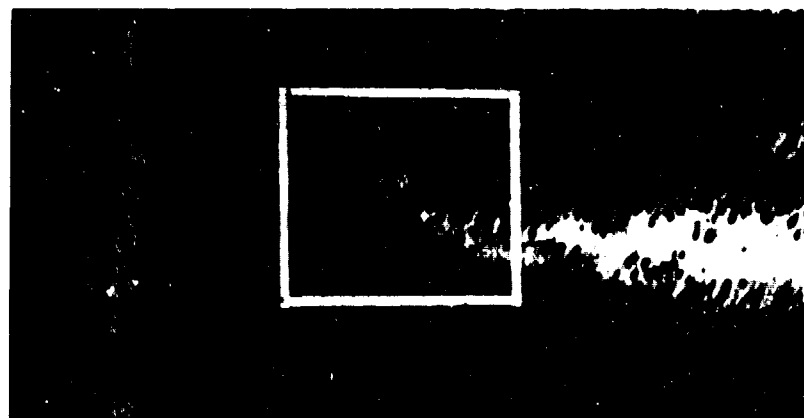


.2μ

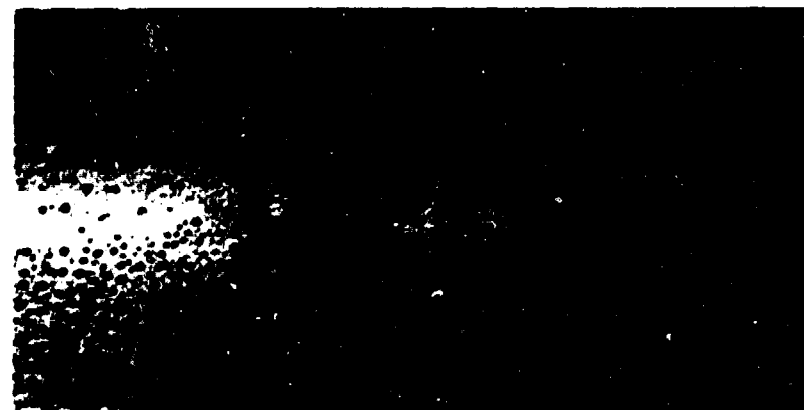




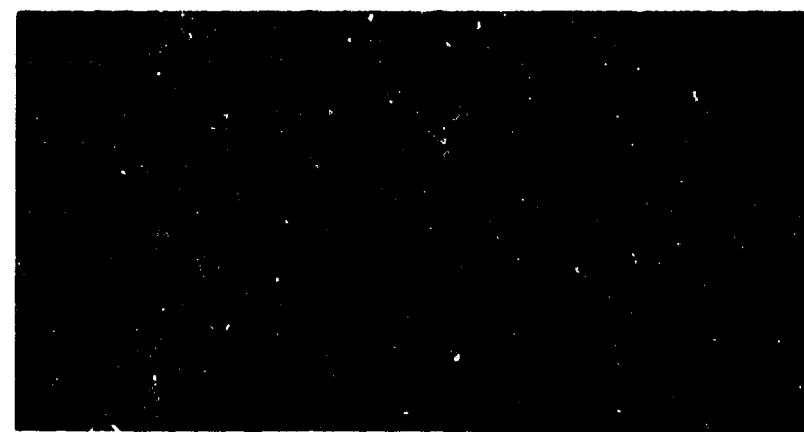
7A



7B



7C



7D

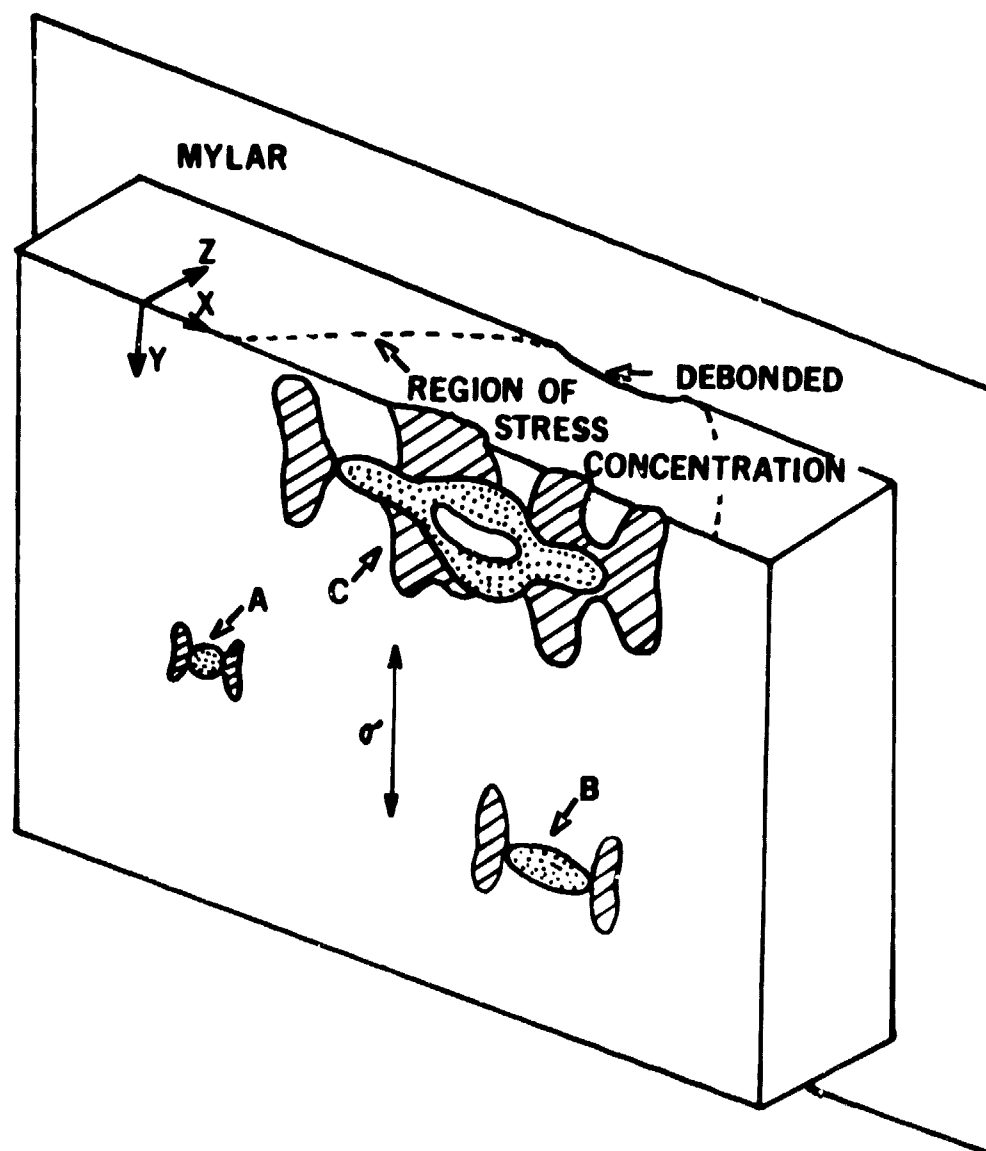
$.1\mu$



7E

 SEVERE MICRONECK

 DIFFUSE YIELD



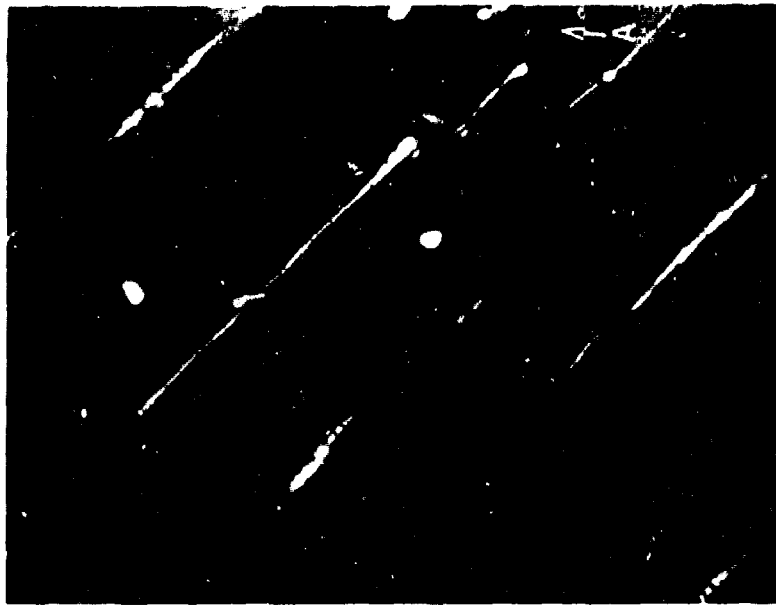


11'



hr

11A



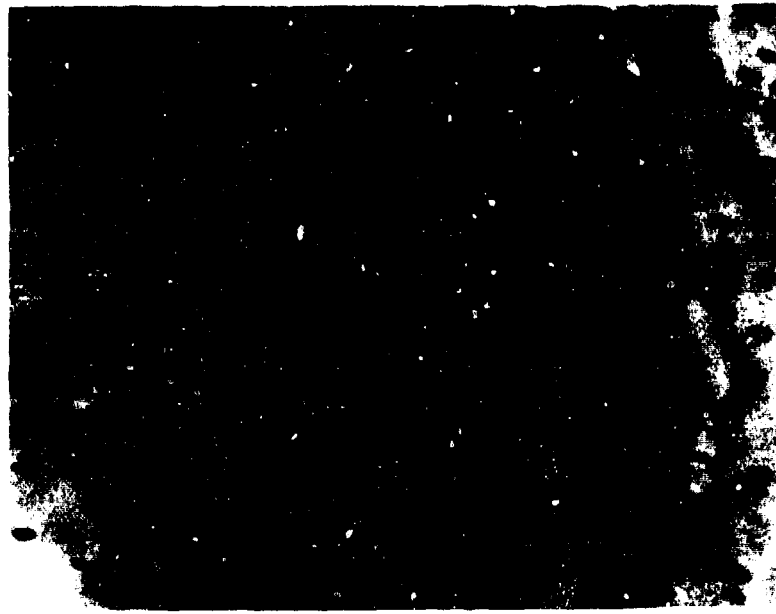
.5μ

11B

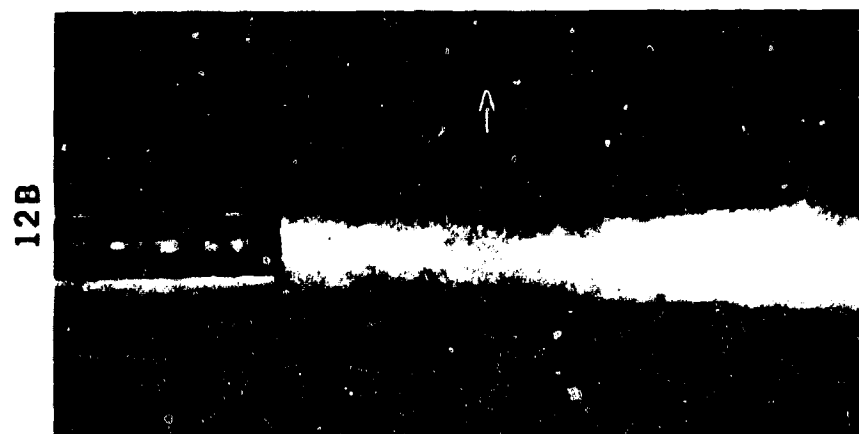
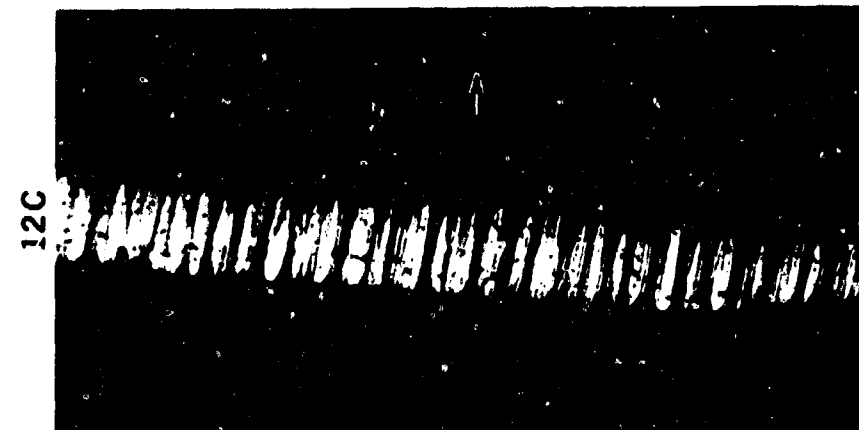


.2μ

11C



.5μ

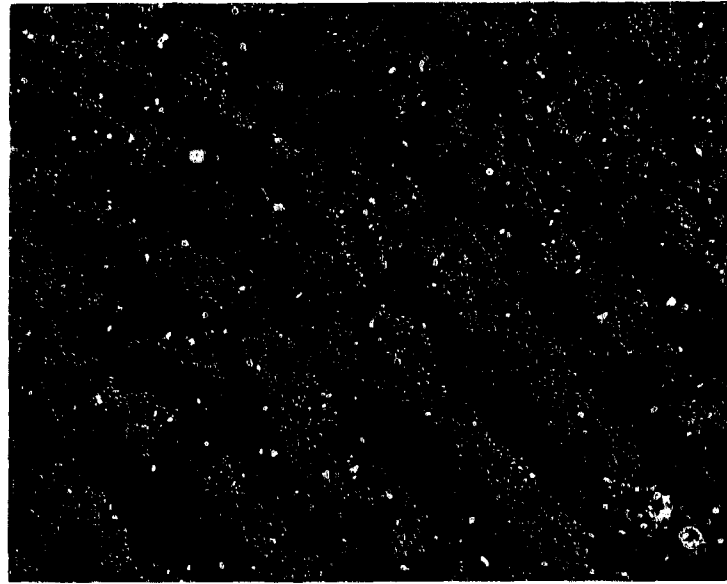


.2μ

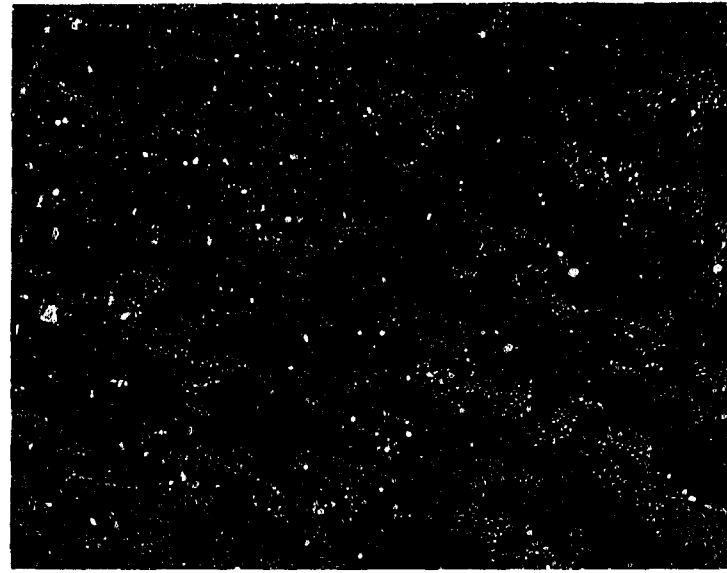


Reproduced from  
best available copy.

13A



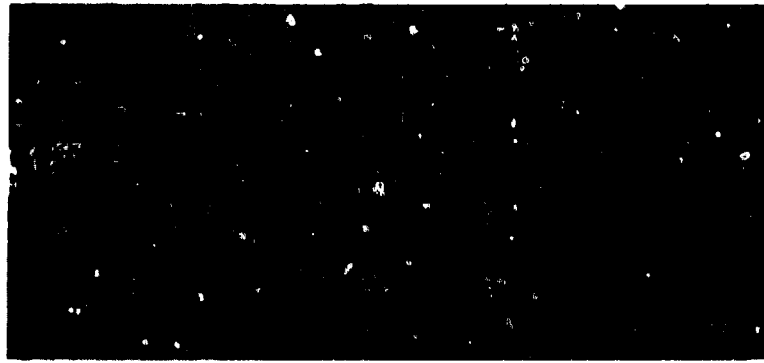
13B



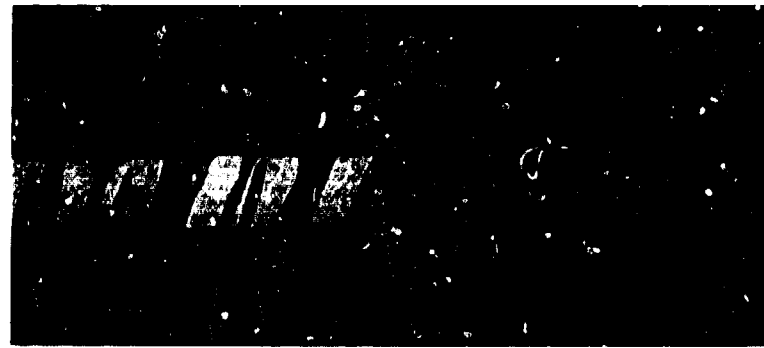
.2μ



14A



14B



.3μ

14C



14D

